Stanford Exploration Project, Report 120, May 3, 2005, pages 395–406

Removal of linear events with combined radon transforms

Brad Artman and Antoine Guitton[1]

ABSTRACT

We explore the classic signal and noise separation problem of removing linear events from shot-gathers through several inversion schemes using a combined modeling operator composed of both hyperbolic and linear radon transforms. Data are inverted simultaneously for both linear and hyperbolic moveout which provides two model-space outputs. These are forward modeled seperately to provide an output data-space devoid of one of the model-space components. We employ this approach to analyze the removal of direct arrivals and ground-roll from shot-gathers. Inversion schemes used imnclude: 1) bound-constrained, 2) Cauchy norm regularization, 3) Huber norm approximating the l_1 norm, and 4) the l_2 norm using linear least-squares. Synthetic tests and four field shot-gathers are used to demonstrate the approach. Methods 1, 2, and 3 are designed to provide sparse model-space inversions. In the real data examples, the least-squares solution is able to better achieve the signal to noise separation goal despite its model-space being often less appealing.

INTRODUCTION

Chen et al. (1999) introduces the idea that inversion problems solved with a sparseness constraint on the output model-space can be applied to data sets with an over-complete modeling operator. Over-complete means that the dictionary of transform kernels has (many) more terms than a strict basis transformation such as the standard DFT. For example, this could be realized by using several different modeling operators or even a over-sampled version of a single operator such as a Fourier transform with several times more frequency resolution than the compact support definition of DFT theory. Further, in Donoho and Huo (1999) the mathematics are presented to prove that the combined suite of model space kernels are orthogonal to each other if the inversion satisfies several requirements. Their goal is super-resolution during the analysis of a signal. These investigations are presented within the framework of inversion through linear programming techniques. Futher, the papers imply that these desirable properties are realized with the use of an inversion methodology using a l^1 norm on the model-space. Artman and Sacchi (2003) made preliminary efforts to investigate these properties, but were stalled due to the instability and expense, when applied to the much larger and more complicated data domains of seismic data, of the linear programming technique. Trad et al. (2003) present results of such a combined operator inversion scheme using the Cauchy regularization.

[1]**email:** brad@sep.stanford.edu, antoine@sep.stanford.edu

Guitton (2004) explores the novel result that two bound-constrained inversions (bounded by zero from below and above) contain orthogonal null-spaces. Therefore, summing the results of two such inversions can significantly enhance the sparseness of the model space compared to that produced by an inversion which is free to output both positive and negative values for the inverted model. The cost for this improvement is an extra inversion of identical size and cost. This characteristic is shared with the linear programming techniques used for the super-resolution problem, though the inversion algorithm is the L-BFGS.

We will compare the inverted models from several inversion schemes, and their concomitant data-space realizations. Inversion schemes that will be analyzed are:1) bound-constrained (BC), 2) Cauchy norm regularization (Cauchy), 3) Huber norm approximating the l_1 norm (l_1), and 4) the l_2 norm using linear least-squares (l_2). The combined operator of Hyperbolic and Linear Radon Transforms will be used in all the inversion schemes on both synthetic data and three field shot gathers.

THEORY

The addition of a second simultaneous linear operator expands the usual linear inversion equations to the slightly more complicated linear operator (Claerbout, 1999),

$$\mathbf{L} = [\mathbf{L}_1 \, \mathbf{L}_2]$$

and a correspondingly longer model vector

$$\mathbf{m} = \left[\frac{\mathbf{m}_1}{\mathbf{m}_2} \right] .$$

This simple introduction leads to the form of the inversion goals used here

$$[\mathbf{L}_h \mathbf{L}_l] \left[\frac{\mathbf{m}_h}{\mathbf{m}_l} \right] = \mathbf{d} \tag{1}$$

$$\epsilon^2 \mathbf{I} \left[\frac{\mathbf{m}_h}{\mathbf{m}_l} \right] = 0 \, , \tag{2}$$

where subscripts h and l refer to the hyperbolic (HRT) and linear (LRT) radon transforms and we add identity operator regularization to provide damping.

SYNTHETIC EXAMPLES

The first concern when solving inversion problems with over-complete dictionaries is the potential for introduction of cross-talk (Claerbout, 1992) into the model-space. A synthetic data set was created to test the method to assure that this technique does not allow this to happen. Figure 1 shows the inverted models produced with the various methods compared to the least-squares solution. The first panel is a bandlimited model from which data were forward modeled, and the last four panels show the models produced by the various inversion procedures.

While the first two inversion schemes produce very sparse model-spaces with no cross-talk, the l_1 and l_2 products contain the familiar parabolas in the LRT domain due to data-space hyperbolas and ellipses in the HRT domain from the linear events in the data.

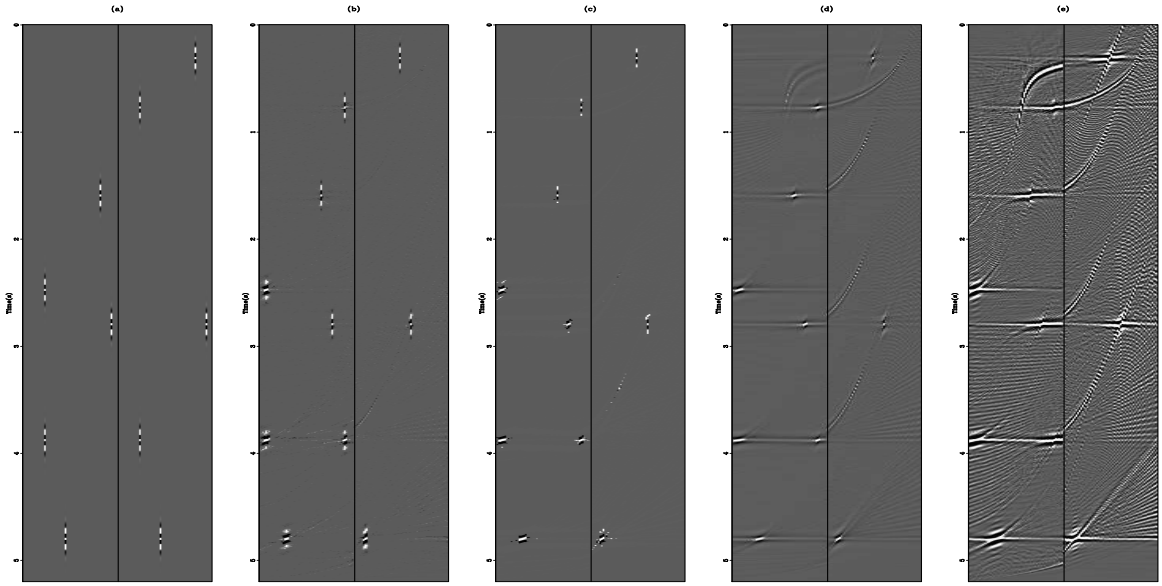

Figure 1: Synthetic model-space examples. The model-space contains both radon domains. Thus, half way across the slowness axis the plot changes from representing energy in the hyperbolic radon domain to events in the linear radon domain. The origin and sampling interval for both domains are the same in this example. Panel (a) is the band-limited model. Panel (b) shows the BC inversion result. Panel (c) shows the Cauchy result. Panel (d) shows the l_1 result. Panel (d) shows the l_2 result. brad2-syn1 [CR]

The models produced by all the results are very good. The clip level is deliberately set very low to bring out artifacts. While the first two methods produce very sparse results, the l_1 and l_2 results contain sweeping artifacts and readily identifiable cross-talk between the two model domains.

Figure 2 shows the forward modeled data from the models produced from the various inversion techniques. The first panel is the starting data. Once again, the clip level has been set quite low to bring out the artifacts of the latter inversion schemes. Amazingly, the two sparse inversion schemes, especially the Cauchy inversion in panel (c), were able to remove much of the 0.000001 variance noise added to the data. A small amount of corrilary chatter can be seen in the Cauchy, l_1, and l_2 data domains linear.

The inversion schemes designed for sparse model domains have produced models with no cross-talk between the two operators. The l_1 and l_2 inversions have allowed the transmission of energy between the two domains. However, the forward modeled data from all the methods show more than adequate results with only minor noise introduced in the immediate vicinity of the various events. Importantly, even the very steeply dipping events are well modeled despite being severely aliased. It should be noted however, that the first two schemes will not produce

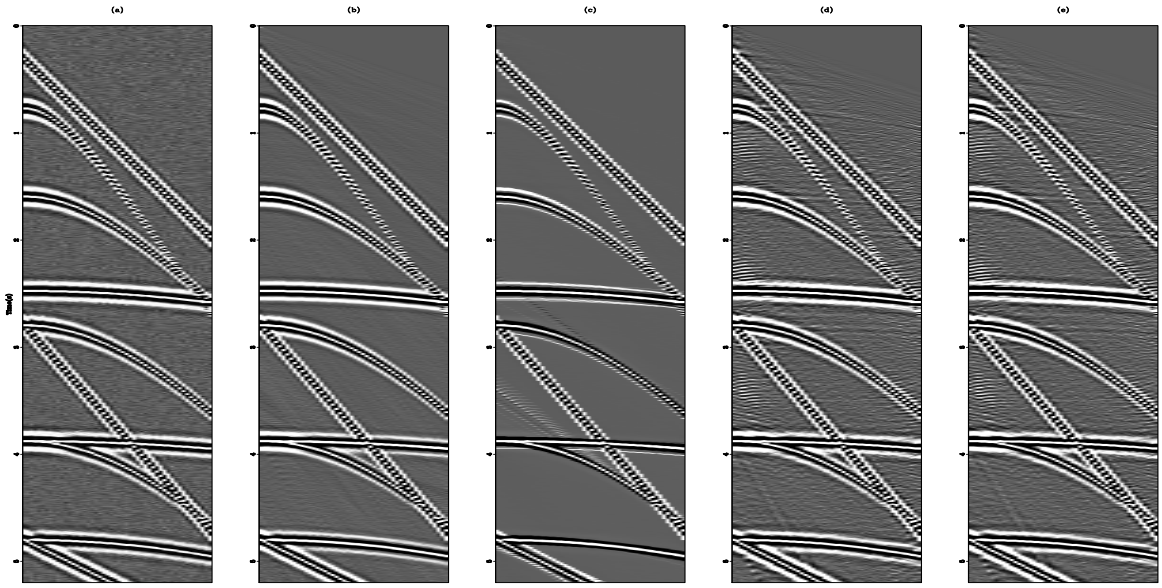

Figure 2: Forward modeled data from the inversion results presented in Figure 1. Panel (a) is the band-limited model. Panel (b) shows the BC inversion result. Panel (c) shows the Cauchy result. Panel (d) shows the l_1 result. Panel (d) shows the l_2 result. brad2-syn2 [CR]

satisfactory data-space results given realistic split-spread gathers. Their short-comings are from linear events that do not continue completely across the entire data domain. The sparse model domains do not have sufficient freedom to add fictitious model energy to cancel events that do not exactly eminate from the origin of the shot (*ie.* exit the gather at $t = 0, x = 0$). Throughout this effort, only off-end gathers will be used.

NOISE SEPARATION IN FIELD DATA

Four shot-gathers are used to explore the efficacy of this method to remove linear events from shot-gathers. The paradigm is that linear events due to direct arrivals and ground-roll are noise and hyperbolic events due to subsurface reflectors should be maintained. The simple approach is to forward model only the linear model-space which can will then be directly subtracted from the data.

Figure 3 shows the data examples that will be used. They are shots 08, 14 and 25 from the Yilmaz shot-gathers. The three examples contain a nice compilation of common land data artifacts to be attacked through the removal of linear events. Direct arrivals, refractions, and ground-roll are all experienced to some degree both at early time and obscuring primaries late in the sections. A strong linear wavetrain dominates the early time of shot 08, Panel (a). Shot 14, Panel (b), has faint linear events at late time and several slopes at early time. The non-hyperbolic moveout at 5.2 seconds is a nice marker for judging the quality of the various inversion schemes. The obvious ground-roll in shot 25, Panel (c), is the main goal to eliminate.

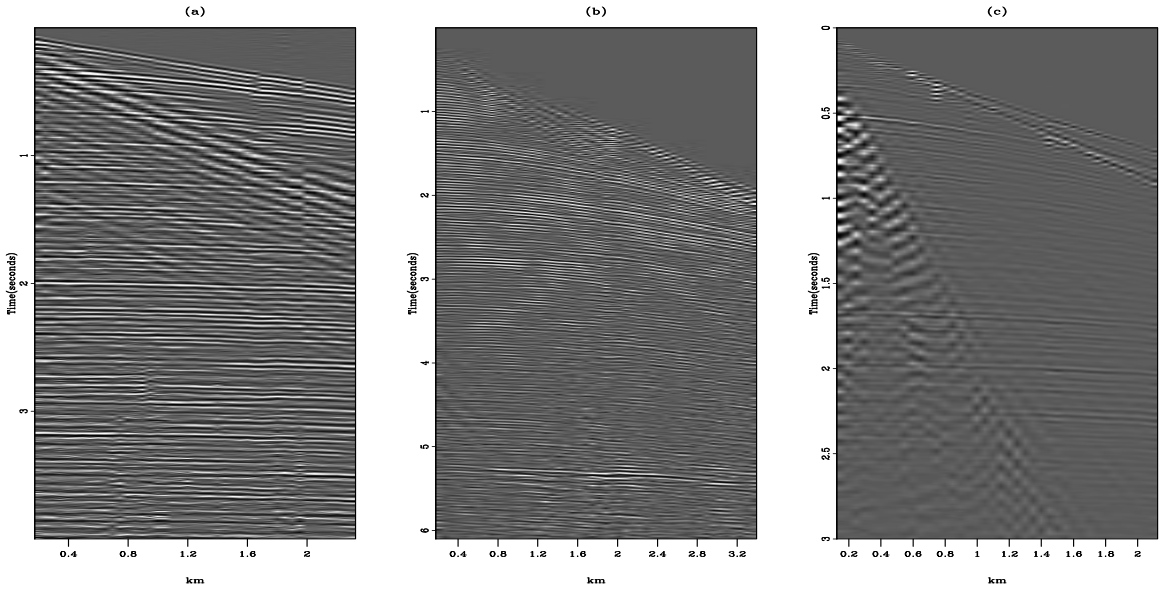

Figure 3: Shots from the Yilmaz data collection. Panel (a) is shot 08, Panel (b) is shot 14, Panel (c) is shot 25. brad2-d [ER]

Radon domain

Figure 4 through 6 contain the inverted model domains associated with the four techniques explored herein. Clearly the sparsity of the results decrease toward the right. Direct interpretation of the model domain would be easier and more accurate with the BC, Cauchy, and l_1 results. Distict trains of energy in the hyperbolic and linear domains are visible. Without the clip set so low, the l_2 result is not as bad as these panels make it seem. A distinct fairway of energy, marginally larger than that presented in the l_1 result is visible. Velocity analysis of the gathers would likely be more accurate with the results that impose sparsity, especially at late times.

In general the l_1 inversion produced consistantly better model space realizations. While the differences are often minor, the method provides consistant, stable, high quality results.

Data residuals

The data-space residuals of the inversion schemes are presented in Figures 7 through 9. The clip level in all cases are the same as the data in Figure 3. The sparse model-spaces produce residual panels less like the original data than the l_2 norm inversion. This results in data residuals often indistinguishable from the original data to the eye for the sparse schemes.

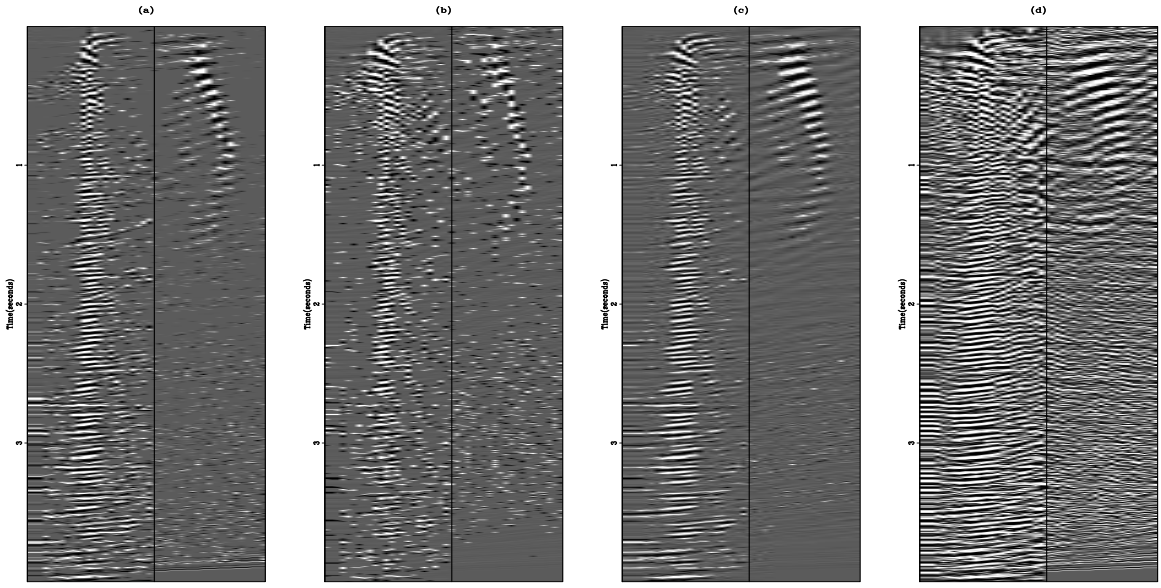

Figure 4: Model-space inversions of shot-gather 08 (Panel (a) from Figure 3). The first half of the panels is HRT space and the second half is LRT space. Panel (a) shows the BC, Panel (b) the Cauchy, Panel (c) the l_1, and Panel (d) the l_2 inverted model spaces. brad2-m.08 [ER]

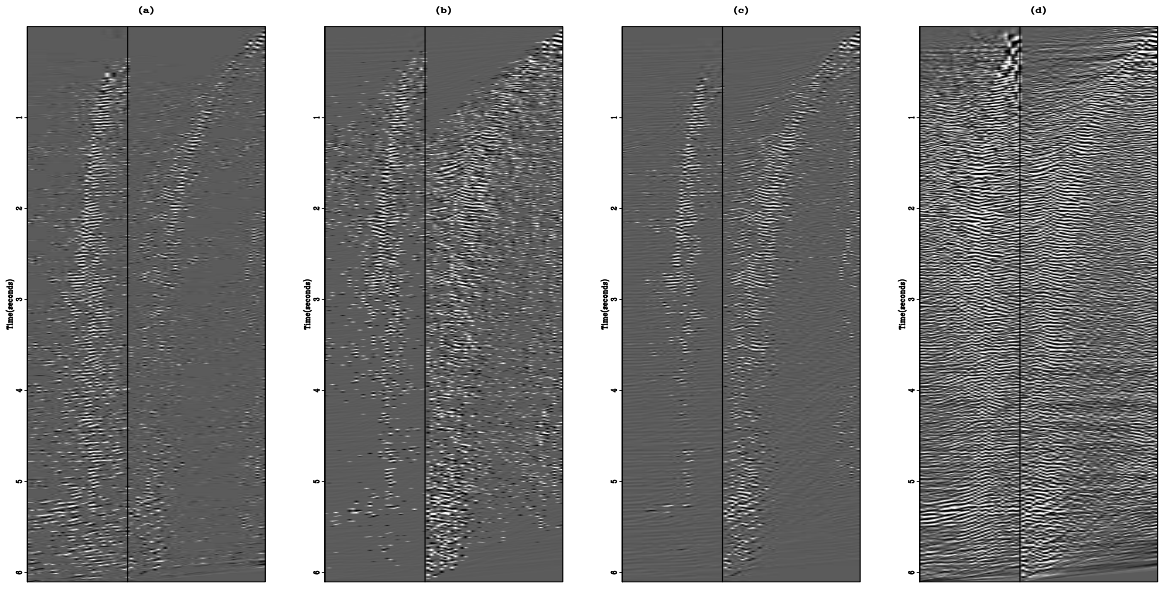

Figure 5: Model-space inversions of shot-gather 14 (Panel (b) from Figure 3). The first half of the panels is HRT space and the second half is LRT space. Panel (a) shows the BC, Panel (b) the Cauchy, Panel (c) the l_1, and Panel (d) the l_2 inverted model spaces. brad2-m.14 [ER]

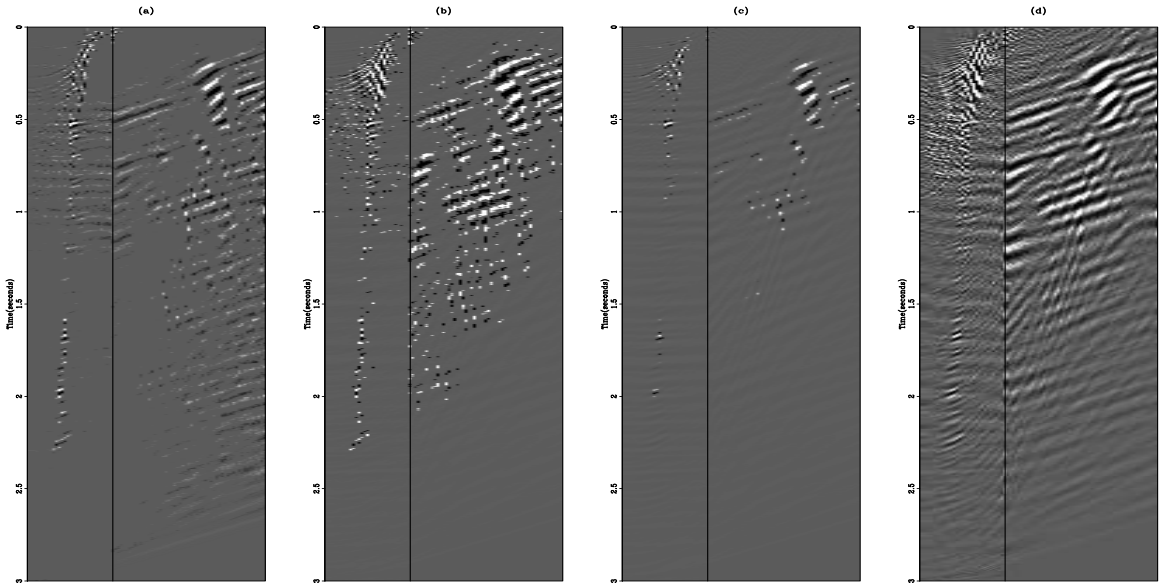

Figure 6: Model-space inversions of shot-gather 25 (Panel (c) from Figure 3). The first half of the panels is HRT space and the second half is LRT space. Panel (a) shows the BC, Panel (b) the Cauchy, Panel (c) the l_1, and Panel (d) the l_2 inverted model spaces. brad2-m.25r [ER]

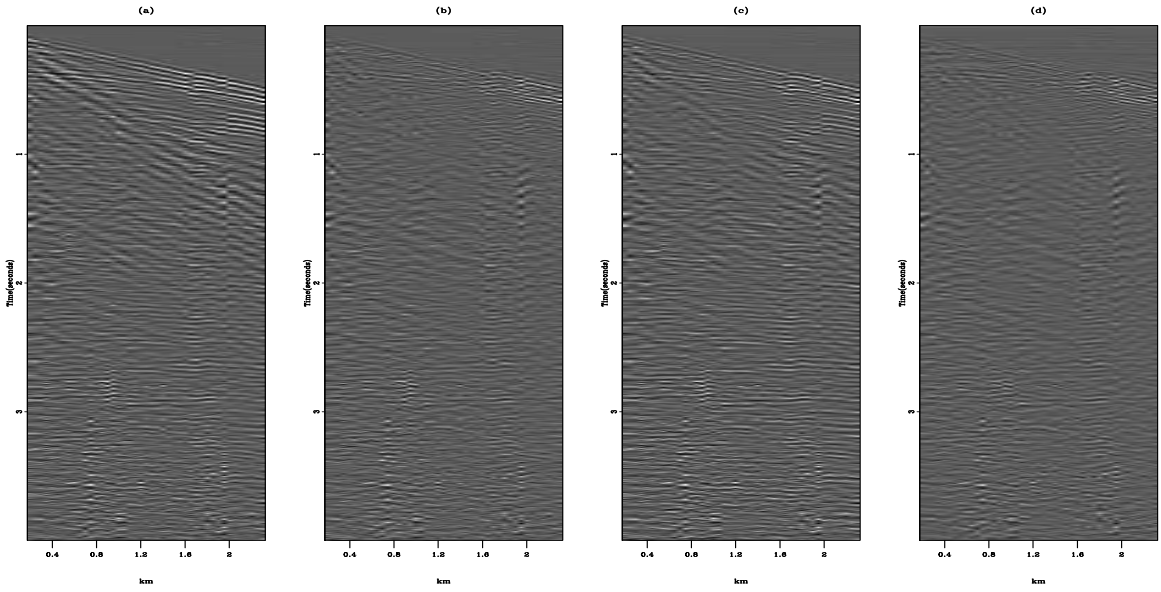

Figure 7: Data-space residuals of shot-gather 08 (Panel (a) from Figure 3). Panel (a) shows the BC, Panel (b) the Cauchy, Panel (c) the l_1, and Panel (d) the l_2 inversion results. brad2-r.08 [ER]

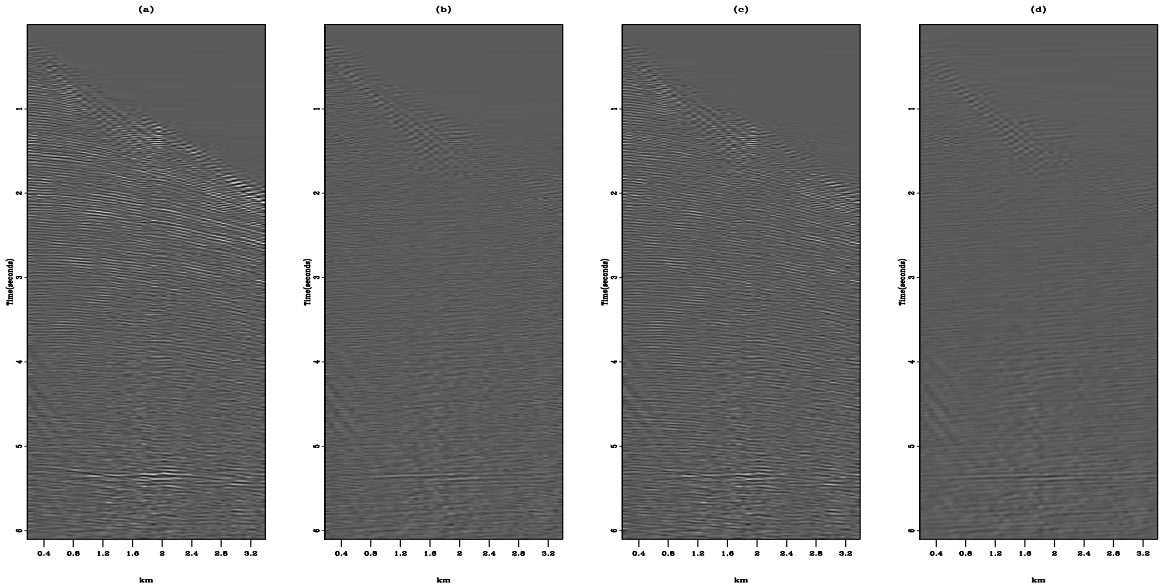

Figure 8: Data-space residuals of shot-gather 08 (Panel (b) from Figure 3). Panel (a) shows the BC, Panel (b) the Cauchy, Panel (c) the l_1, and Panel (d) the l_2 inversion results. brad2-r.14 [ER]

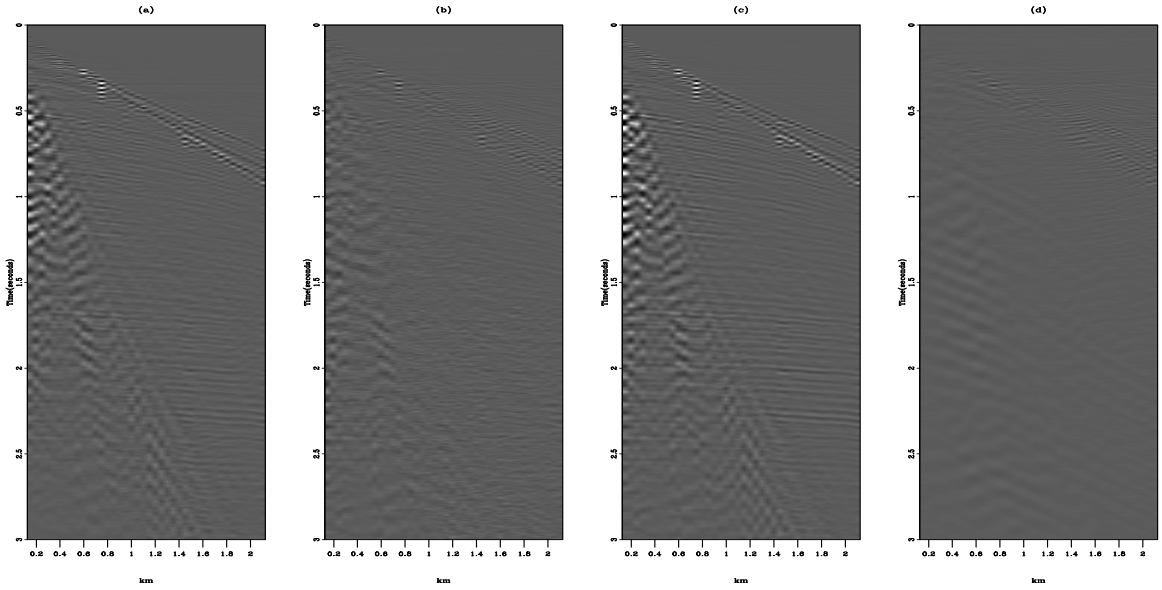

Figure 9: Data-space residuals of shot-gather 08 (Panel (c) from Figure 3). Panel (a) shows the BC, Panel (b) the Cauchy, Panel (c) the l_1, and Panel (d) the l_2 inversion results. brad2-r.25r [ER]

Noise subtraction

Figures 10 through 12 show the efficacy of this simple signal to noise subtraction algorithm facilitated by the combined modeling operator inversion scheme presented here. Only the LRT model-space is forward modeled back into the data-space for subtraction from the original data. In every case the least-squares approach produces the best signal enhancement. Gather 14 produces a lot of acausal noise that could be muted, though the direct arival was the main target for this gather. That being the case, it could also be considered a poor result.

The sparesness oriented schemes produce gathers with little to no improvement in signal-to-noise ratio while altering the amplitude variation, and sometimes kinematics, of the gathers.

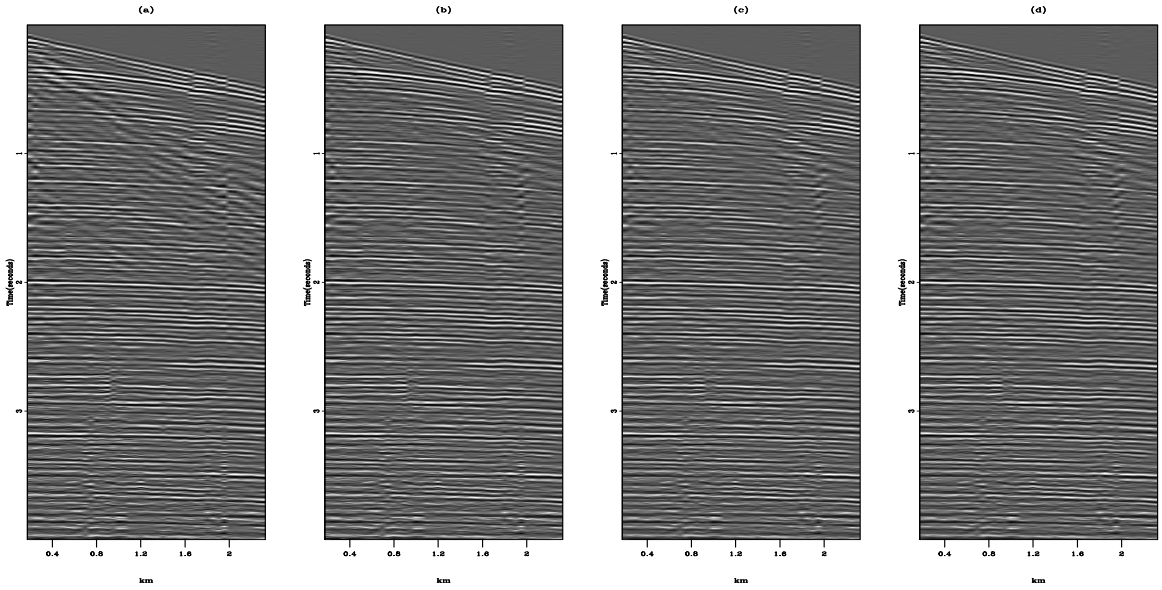

Figure 10: Signal estimate for shot-gather 08 (Panel (a) from Figure 3). Panel (b) shows the BC, Panel (c) the Cauchy, Panel (d) the l_1, and Panel (d) the l_2 inversion results. brad2-s.08 [ER]

COMMENTS AND CONCLUSIONS

It will be noted that because the ground roll is very aliased and dispersive in these gathers, the linear radon operator has great difficulty describing these events with a single kernel in the model domain. While the least squares inversion will introduce energy into the model-space to combine these events, as well as cancel acausal energy above the direct arrival in the data-space, the sparse inversions are not capable of stopping events that do not cross the entire data-space. For this reason, only one-sided gathers have been used for this analysis.

These techniques are particularly sensitive to noisy, unbalanced traces. For this reason all gathers have been trace-balanced, gained as a function of time, and noisy traces zeroed. Last,

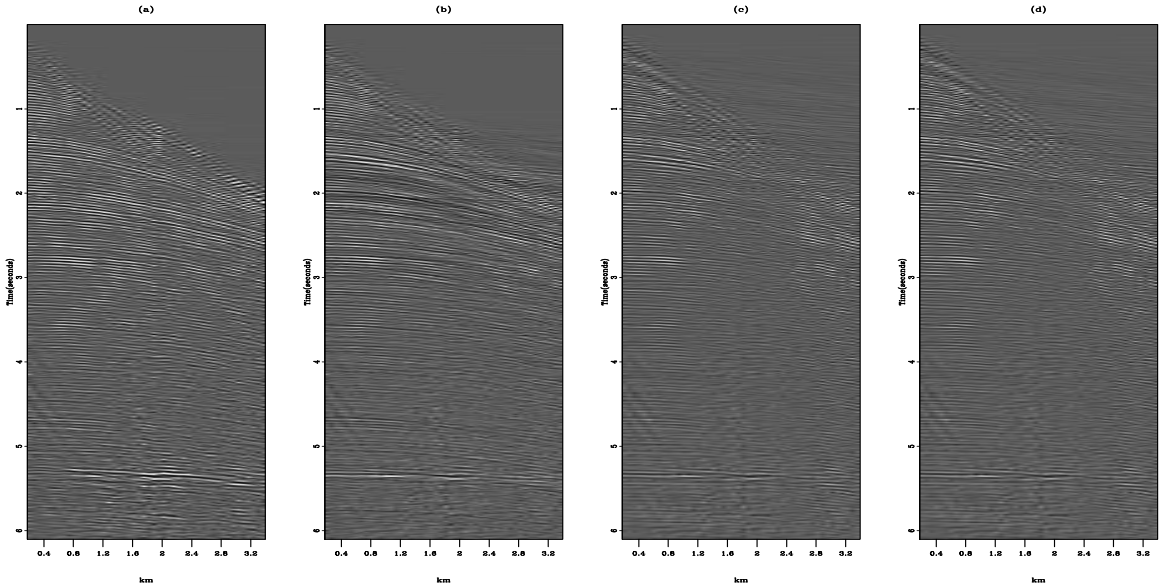

Figure 11: Signal estimate for shot-gather 14 (Panel (b) from Figure 3). Panel (b) shows the BC, Panel (c) the Cauchy, Panel (d) the l_1, and Panel (d) the l_2 inversion results. brad2-s.14 [ER]

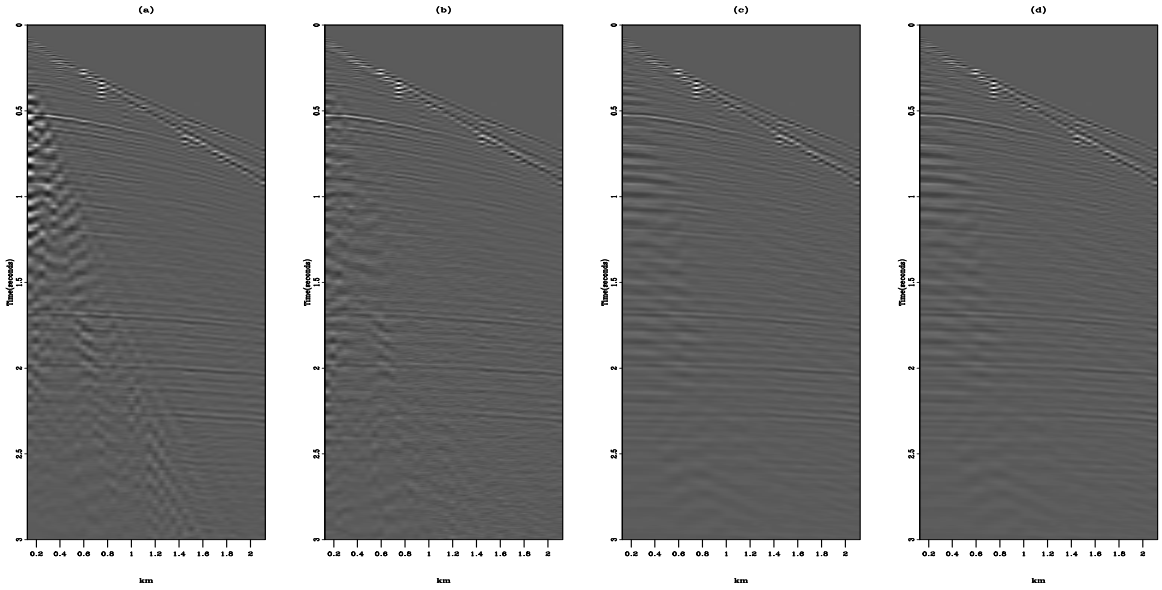

Figure 12: Signal estimate for shot-gather 25 (Panel (c) from Figure 3). Panel (b) shows the BC, Panel (c) the Cauchy, Panel (d) the l_1, and Panel (d) the l_2 inversion results. brad2-s.25r [ER]

it should be noted that CMP-gathers should be used for this analysis instead of shot-gathers to insure that all of the subsurface hyperbolas do not have an apex shift.

While the bound-constrained, Cauchy, and l_1 inversion schemes produce a more pleasing model-space, this investigation shows it is of limited use in this application of separating the linear from hyperbolic events in a CMP gather. While the least-squares inversion does allow the introduction of cross-talk between the two model-spaces, the noise subtraction technique is better implemented within this framework. This conclusion can be evaluated in terms of the sometimes disparate goals of analysis versus synthesis. If analysis is the goal, the sparseness optimized inversion schemes clearly outperform the least-squares model product. Velocity picking would be much better performed with these results. Of the three, this exploration shows the l_1 scheme to be more tolerant in terms of the combined ease of parameter selection and quality of the model-space. For noise (linear event) separation, the least-squares solution enjoys both a high quality result and tolerance in terms of parameter selection. Further, the least-squares solution is much faster and requires fewer iterations. Purposefully halting the inversion after less than 30 iterations was important to avoid the inversion making efforts to fit the noise in the data. However, to realize a sparse model domain, at least 100 iterations were required for the other, slower, techniques. Full investigation into the ramifacations of prematurely stopping the sparse inversion schemes was not performed.

For the purpose of removing linear events with a combined HRT-LRT inversion scheme a data-space solution is required. For this problem, the extra expense of fine-tuning the model-space is wasted.

REFERENCES

Artman, B., and Sacchi, M., 2003, Basis pursuit for geophysical inversion: SEP–**114**, 137–150.

Chen, S. S., Donoho, D. L., and Saunders, M. A., 1999, Atomic decomposition by basis pursuit: SIAM Journal on Scientific Computing, **20**, no. 1, 33–61.

Claerbout, J. F., 1992, Earth Soundings Analysis: Processing Versus Inversion: Blackwell Scientific Publications.

Claerbout, J., 1999, Geophysical estimation by example: Environmental soundings image enhancement: Stanford Exploration Project, `http://sepwww.stanford.edu/sep/prof/`.

Donoho, D., and Huo, X. Uncertainty principles and ideal atomic decomposition:. WWW, citeseer.nj.nec.com/donoho99uncertainty.html, June 1999. NSF grants DMS 95-05151 and ECS-97-07111.

Guitton, A., 2004, Bound constrained optimization: application to the dip estimation problem: SEP–**117**, 51–62.

Trad, D., Ulrych, T., and Sacchi, M., 2003, Latest views of the sparse Radon transform: Geophysics, **68**, no. 1, 386–399.